Original Research

Normative intercapillary distance and vessel density data in the temporal retina assessed by wide-field spectral-domain optical coherence tomography angiography

Keke Liu[1,2], Yukun Guo[1] , Qisheng You[1], Tristan Hormel[1] , Thomas S Hwang[1] and Yali Jia[1,3]

[1]Casey Eye Institute, Oregon Health & Science University, Portland, OR 97239, USA; [2]John A. Burns School of Medicine, University of Hawai'i, Honolulu, HI 96813, USA; [3]Department of Ophthalmology and Biomedical Engineering, School of Medicine, Oregon Health & Science University (OHSU), Portland, OR 97239, USA
Corresponding author: Yali Jia. Email: jiaya@ohsu.edu

Impact statement

In this paper, we describe the normative trends and associations of frequently used perfusion metrics in the far temporal region of the retina. Recently, there has been an increasing focus on larger fields of view in OCT angiography (OCTA) technology. However, to accurately measure abnormal characteristics, it is necessary to accurately characterize normative parameters. This study provides information on the distribution of both vessel density (VD) and intercapillary distance (ICD) in three retinal plexuses/complexes: the superficial vascular complex, ganglion cell layer plexus, and deep vascular complex. En face color maps are provided to visualize the noticeable decrease in VD and increase in ICD towards the far temporal region. Transverse angiographic analyses provide meaningful information on how VD and ICD quantitatively change with increasing distance from the fovea. This new information will inform future studies to more accurately characterize pathologic regions with more confidence.

Abstract

A limitation of conventional optical coherence tomography angiography (OCTA) is the limited field of view normally used in data acquisition. As the technology improves, larger fields of view that capture information away from the macular are being explored in order to provide an enhanced ability to detect pathology. However, normative measurements for important OCTA metrics like vessel density and intercapillary distance are not currently well-characterized in the peripheral retina. In this prospective study, we measured vessel density and intercapillary distance of the superficial vascular complex, ganglion cell layer plexus, and deep capillary plexus in montaged macular/temporal scans from 53 (33 men) healthy volunteers. Vessel density and intercapillary distance were also compared across different regions of the retina, including along arcs at separate distance from the fovea. Compared to the central macular region, the temporal retina had significantly lower vessel density, decreased thickness, and greater intercapillary distance in the superficial vascular complex, GCLP ganglion cell layer plexus, and deep capillary plexus (Wilcoxon rank sum test $P < 0.001$), with each of the plexuses examined here showing a general decrease in vessel density and an increase in intercapillary distance towards the temporal region. No significant difference was noted comparing corresponding vessel density and intercapillary distance regions above and below the macula, and multiple linear regression showed that age and intraocular pressure were not associated with vessel density and intercapillary distance in most models. Repeatability analysis reported as intraclass correlation coefficients demonstrated moderate to excellent reliability of vessel density and intercapillary distance in all OCTA layers. These results should help provide an enhanced baseline to help identify vascular pathology in the peripheral retina.

Keywords: Anatomy, bioimaging, biology/physiology, imaging, medical, ophthalmology

Introduction

Optical coherence tomography angiography (OCTA) has become a widely used retinal imaging modality. Numerous studies have demonstrated its utility in identification and monitoring of many retinal diseases including age-related macular degeneration, diabetic retinopathy, and retinal vein occlusion.[1–3] The ability to objectively evaluate retinal disease through quantification of

vascular metrics has generated much interest.[4] Of these, vessel density[5,6] (VD) and nonperfusion area[7,8] (NPA) are two of the most frequently used metrics employed to evaluate retinal vascular disease.[9–11]

The majority of VD and NPA studies in OCTA have been performed using central 3 × 3 mm centered on the macular. This small field of view is a limitation of conventional OCTA imaging. Wide-field OCTA can visualize more peripheral pathologies that may be missed by smaller fields of view and enable quantification of more vascular changes.[12,13] Such quantification has the capacity to improve OCTA-aided diagnosis, but the vasculature of a healthy eye as seen by OCTA in peripheral regions remains poorly characterized. While it is known that vascular density varies in different regions of the retina, normative data of vascular metrics as measured by OCTA in the periphery are limited. To understand VD and NPA as abnormal, it will be helpful to establish a normative distribution of VD and intercapillary distance (ICD, frequently used for detecting NPA[14,15]).

You *et al.*[16] previously reported on the macular vessel density in a large cohort of 1631 eyes, but the OCTA image was centered only on the macula without information from the temporal periphery. More recently, Lavia *et al.*[17] investigated a small sample of 10 eyes from 10 healthy subjects using several 3 × 3 mm montages from a swept-source OCTA (SS-OCTA) machine and reported capillary density variation in four retinal sectors.

In this study, we characterize the normative perfusion metrics from larger 6 × 6 mm scans of the retina, including the field immediately temporal to the scan centered on the fovea. We quantify these metrics by radial distance from the fovea. We further angle with the horizontal by comparing perfusion metrics along arcs. This fine-grained approach allowed us to more fully characterize small scale variation than previous work. We further used statistical tests to both test for significance of observed perfusion variation and to characterize the association of perfusion parameters with other potentially influencing factors such as retinal thickness, age, and OCT signal strength.

## Materials and methods

Study population

We recruited healthy volunteer participants from Casey Eye Institute for this study, which was approved by the Oregon Health & Science University institutional review board and complied with the Declaration of Helsinki and HIPAA regulations. All participants provided written informed consent at enrollment. They underwent a medical history inquiry, comprehensive clinical examinations, and ocular imaging. The clinical examinations included Early Treatment of Diabetic Retinopathy Study (ETDRS) protocol visual acuity, intraocular pressure, slit-lamp biomicroscopy, and indirect binocular ophthalmoscopy. Imaging procedures included dilated color fundus photography and OCTA. The exclusion criteria were as follows: retinal pathology, diagnosis of glaucoma, systemic disorder impacting the eye, history of ocular surgery, or medical treatment for an ocular condition. Further exclusion criteria based on image scans included signal strength index (SSI) < 50, large motion artifacts, strong shadow artifacts (e.g. a shadow caused by an eyelash, vitreous floaters, or pupil vignetting), defocusing, failure to complete the scan, and arcs with missing data from more than half of the participants.

Data acquisition and segmentation boundaries

One eye of each healthy subject underwent high-definition (400 × 400-pixel) 6 × 6-mm OCTA scans centered on the fovea and temporal retina consecutively with ∼0.5 mm overlap (Figure 1) using a commercially available SD-OCTA system (Avanti RTVue-XR, Optovue Inc.). Mean arterial pressure was calculated as 2/3 × [diastolic blood pressure] + 1/3 × [systolic blood pressure]. The intraocular pressure was measured with Goldman tonometry.

A guided bi-directional graph search algorithm[18] was used to segment seven retinal boundaries, from which maximum projection[19] was used to produce *en face* images of the superficial vascular complex (SVC), ganglion cell layer plexus (GCLP), and deep capillary plexus (DCP). Definitions of the OCTA *en face* angiograms were: GCLP:
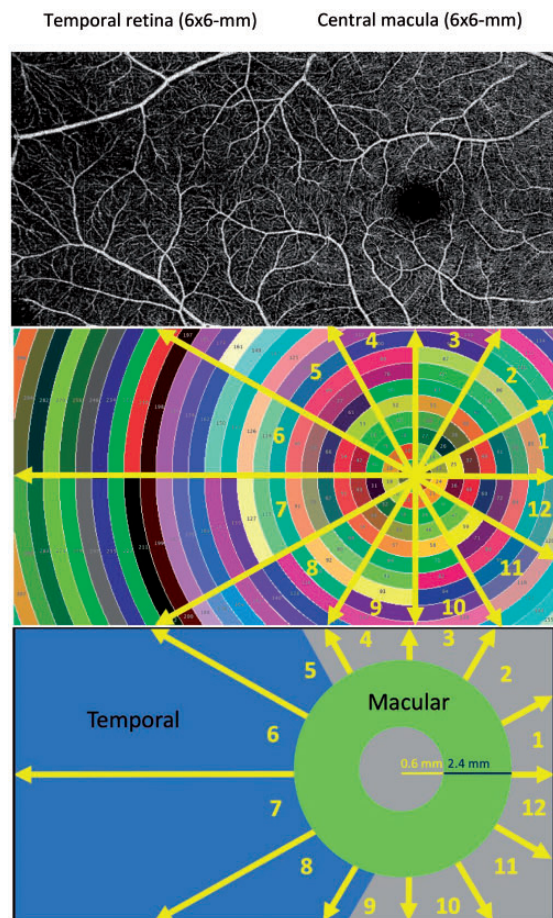
Figure 1. (Top) Montaged 6 × 6-mm OCTA scans showing the fovea and temporal retina. (Middle) Sectored map of the macular and temporal regions. (Bottom) Definition of temporal (blue) and macular (green) regions. (A color version of this figure is available in the online journal.)

67% of combined ganglion cell and inner plexiform layer (GCIPL); SVC: nerve fiber layer (NFL) and GCLP; DCP: 50% of inner nuclear layer (INL) in addition to the outer plexiform layer (OPL, Figure 2.)[4] We anticipated that VD and ICD may vary with the thickness of the layers in which they are embedded, so the thicknesses of these layers were also measured from the segmented retinal slabs.[4,20] The vascular slabs as defined above were chosen in order to provide clean images of the plexuses in isolation. However, they do not correspond to the anatomic regions perfused by the retinal plexuses. The thickness measurements reported here therefore are taken over the entire associated retinal slabs instead of the fractional slabs used for projection (i.e. the entire rather than partial GCIPL and INL).

Image analysis

Vessel density (VD) was calculated as the percentage of pixels with flow signal in a vascular plexus or complex. To separate the vascular and nonvascular pixels, a threshold of noise was defined as 2.33 standard deviation above the mean decorrelation signal in the foveal avascular zone (FAZ). Intercapillary measures capillary spacing. Specifically, we used a Euclidean distance transform algorithm to compute the ICD. This algorithm assigns the distance to the nearest flow pixel to every pixel in the *en face* image.[21] We applied a deep-learning-based method to detect the shadow-artifact-affected areas in each *en face* image.[22] Regions with detected shadows were excluded from analysis.

To characterize the VD and ICD in relation to their location in the retina, we divided the montaged macular and temporal scans in 30° sectors centered at the fovea, number 1–12 in a counterclockwise fashion (Figure 1). Each angular sector was subdivided into concentric arcs at 0.3 mm increments. We excluded regions within or adjacent to the FAZ, up to 0.6 mm, to limit contribution from the inherent variation in FAZ size in a normal population.[7] We adjusted all images to correct for the effect of axial length on linear magnification. The macular region (green) was defined as a donut ring centered on the fovea with maximum and minimum radii of 3.0 and 0.6 mm, respectively. The temporal region (blue) was defined as the arcs in sectors 5–8

extending beyond the macular region temporally. Lastly, we calculated the ICD and VD on the regions free of artifacts and analyzed the variation to their distance from the foveal center. Furthermore, we performed multiple linear regressions between vascular metrics (VD and ICD, separately) of sectors against other covariates (age, MAP, IOP, thickness, and SSI). In the sectors with significant associations to SSI, a linear correction was applied.

Statistical analysis

Wilcoxon rank sum tests were used to determine statistically significant differences ($P < 0.05$) in VD, ICD, and thickness between the macular and temporal regions. Additionally, Wilcoxon rank sum tests were used to compare corresponding sectors in the superior and inferior hemispheres. Multiple linear regression models were performed to investigate associations of VD and ICD with other demographic (age, MAP) and ocular (IOP, thickness, and SSI) parameters. Pearson correlation coefficients reported the relationship between VD and ICD against distance from the fovea. Lastly, a repeatability analysis between the first and second measurements using a subset of the data was conducted using intraclass correlation coefficients (two-way mixed-effects model). All statistical analysis was conducted in R using RStudio (RStudio for mac, version 1.3; PBC, Boston, MA, USA).

Results

Study population

We enrolled 63 eyes from 63 healthy adults (36 men and 27 women) in total and excluded 10 eyes due to a scanning failure where the OCT system cannot acquire valid signals due to strong eye movements. After excluding unqualified subjects, we included 53 eyes from 53 healthy adults (33 men and 20 women; Table 1) in this study. A total of 78 scans were obtained, and 25 scans were used for repeatability testing.

En face color maps of vascular plexuses

ICD, VD, and thickness maps were generated to visually portray the vessel and thickness distributions around the macula (Figure 3). Visually, the DCP slab seems to be

Anatomic layers	Vascular plexuses	Vascular complexes
NFL	NFLP	SVC
GCIPL	GCLP	SVC
GCIPL	ICP	DVC
INL	DCP	DVC
OPL	DCP	DVC

Figure 2. Anatomic (OCT) and vascular (OCTA) definitions. The ganglion cell layer plexus (GCLP) is 67% of GCIPL. DCP is 50% of INL and all of OPL. DCP: deep capillary plexus; DVC: deep vascular complex; GCIPL: combined ganglion cell and inner plexiform layer; GCLP: ganglion cell layer plexus; ICD: intercapillary distance; ICP: intermediate capillary plexus; INL: inner nuclear layer; NFL: nerve fiber layer; NFLP: nerve fiber layer plexus; OPL: outer plexiform layer; SVC: superficial vascular complex; VD: vessel density.

relatively uniform in both the VD and ICD maps. However, in both the SVC and GCLP layers, a decreasing trend in VD and an increasing trend in ICD can be noticed going towards the temporal region. There is also overall symmetry between the superior and inferior regions of the macula.

Regional variation in vascular plexuses

Compared to the central macular 6×6-mm region, the temporal retina had significantly ($P < 0.001$) lower VD and greater ICD in the SVC, GCLP, and DCP (Table 2). As we hypothesized, the thickness was also significantly lower in the temporal compared to the macular region in all three layers. Multiple linear regression showed that in the macular regions of the SVC and GCLP slabs, an increased thickness was correlated with increased VD and decreased ICD (Table 3). In the temporal region, an increase in thickness was only associated with increased VD or decreased ICD in the DCP, not the SVC or GCLP. The signal strength index was not generally correlated with VD or ICD except in the temporal DCP region. Mean arterial pressure was increased with higher VD and lower ICD in the macular region but not the temporal region. In most temporal and macular slabs, age and intraocular pressure were not associated with VD or ICD.

Table 1. Demographic and ocular characteristics of study participants.

Parameter	Mean $\pm$ SD	Range
Participants, *n*	53	
Eyes, *n*	53	
Age (years)	48.2 $\pm$ 17.5	18–78
ETDRS letters	85.7 $\pm$ 5.7	71–97
AL (mm)	23.7 $\pm$ 0.9	21.9–25.8
IOP (mm Hg)	14.3 $\pm$ 2.8	7–24
MAP (mm Hg)	89.5 $\pm$ 9.0	71.7–109.3

AL: axial length; ETDRS: early treatment diabetic retinopathy study; IOP: intraocular pressure; MAP: mean arterial pressure; SD: standard deviation.

Transverse angiographic profiles of retinal vascular plexuses showed a general decrease in VD and an increase in ICD towards the temporal region as captured by sectors 5–8 (Table 4). Regional variation analysis comparing corresponding sectors above and below the macula showed there is no significant difference in most sectors (Table 5).

To investigate the variation of VD and ICD relative to distance from the foveal center, we reported the Pearson correlation coefficients for each sector (Table 6). Nasal progression in the macula (sectors 1, 2, 11, 12) corresponded to an increase in the SVC and GCLP VD and a decrease in ICD. In contrast, temporal progression (sectors 5–8) was associated with a decrease in SVC and GCLP VD and an increase in ICD. Interestingly, in the DCP, both nasal and temporal progression away from the FAZ corresponded to a decrease in VD and an increase in ICD.

Repeatability analysis

Repeat measurements were available in 25 eyes, and the intraclass correlation coefficients demonstrated moderate to excellent reliability of VD and ICD in SVC, GCLP, and DCP layers (Table 7).

Discussion

In this cross-sectional study of healthy participants, we generated normative reference maps to visualize the variation of VD, ICD, and retinal thickness in three major capillary plexuses/complexes: the SVC, GCLP, and DCP. Overall trends in these plexuses toward the temporal periphery include a decrease in VD, an increase in ICD, and a decrease in retinal thickness. Using these maps, we analyzed the changes in these measurements in 12 different directions away from the fovea. Notably, temporal progression in the SVC and GCLP layers corresponded to a larger decrease in VD and increase in ICD compared to the DCP slab. Repeatability analysis on a subset of eyes showed
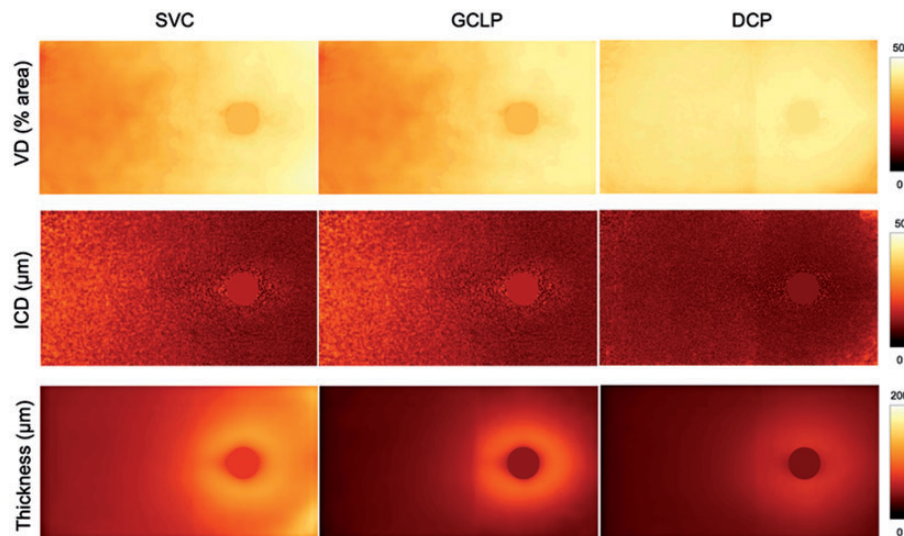
Figure 3. Population averages in key parameters. Images shows average values vessel density (VD), intercapillary distance (ICD), and retinal thickness for the entire study population in the three complexes/plexuses studied in this work: the superficial vascular complex (SVC), deep capillary plexus (DCP), and ganglion cell layer plexus (GCLP). (A color version of this figure is available in the online journal.)

Table 2. Statistically significant differences in all three layers between the macular and temporal regions.

	SVC			GCLP			DCP		
	T	M	*P* value	T	M	*P* value	T	M	*P* value
VD (%)	0.33	0.42	<0.001	0.33	0.42	<0.001	0.21	0.29	<0.001
ICD (mm)	0.029	0.022	<0.001	0.029	0.022	<0.001	0.034	0.029	<0.001
Thickness (μm)	59.6	101.9	<0.001	39.5	68.7	<0.001	37.7	57.4	<0.001

Note: Data reported as mean measurements of temporal and macular regions with Wilcoxon rank sum test *P* value.
DCP: deep capillary plexus; GCLP: ganglion cell layer plexus; ICD: intercapillary distance; M: macular; SVC: superficial vascular complex; T: temporal; VD: vessel density.

Table 3. Multiple linear regression analysis comparing temporal and macular associations to vessel density (VD) and intercapillary distance (ICD) in three layers: superficial vascular complex (SVC), ganglion cell layer plexus (GCLP), and deep capillary plexus (DCP).

Region	Parameter	Vessel density (%)			Intercapillary distance (mm)		
		SVC	GCLP	DCP	SVC	GCLP	DCP
Temporal	Age (years)	$-1.2 \bullet 10^{-4}$	$-1.5 \bullet 10^{-4}$	$-4.9 \bullet 10^{-4}$*	$6.8 \bullet 10^{-6}$	$1.1 \bullet 10^{-5}$	$2.0 \bullet 10^{-5}$
	IOP (mmHg)	$2.2 \bullet 10^{-3}$*	$2.3 \bullet 10^{-3}$*	$-3.4 \bullet 10^{-4}$	$-1.9 \bullet 10^{-4}$*	$-2.0 \bullet 10^{-4}$*	$-3.1 \bullet 10^{-5}$
	MAP (mmHg)	$-3.5 \bullet 10^{-4}$	$-4.1 \bullet 10^{-4}$	$2.7 \bullet 10^{-5}$	$4.8 \bullet 10^{-5}$	$5.2 \bullet 10^{-5}$	$5.8 \bullet 10^{-6}$
	Thickness (μm)	1.32	1.09	3.63**	−0.17	−0.16	−0.30***
	SSI	$4.4 \bullet 10^{-4}$	$3.0 \bullet 10^{-4}$	$2.3 \bullet 10^{-3}$**	$-1.0 \bullet 10^{-4}$	$-8.2 \bullet 10^{-5}$	$-1.6 \bullet 10^{-4}$**
Macular	Age (years)	$-3.5 \bullet 10^{-5}$	$-1.1 \bullet 10^{-5}$	$-1.3 \bullet 10^{-4}$	$4.8 \bullet 10^{-6}$	$2.1 \bullet 10^{-6}$	$2.2 \bullet 10^{-5}$
	IOP (mmHg)	$-1.8 \bullet 10^{-4}$	$-1.3 \bullet 10^{-4}$	$-1.8 \bullet 10^{-4}$	$1.7 \bullet 10^{-5}$	$1.4 \bullet 10^{-5}$	$3.6 \bullet 10^{-5}$
	MAP (mmHg)	$-5.6 \bullet 10^{-4}$**	$-5.4 \bullet 10^{-4}$*	$-6.8 \bullet 10^{-4}$*	$2.8 \bullet 10^{-5}$*	$2.5 \bullet 10^{-5}$*	$4.1 \bullet 10^{-5}$*
	Thickness (μm)	0.93***	1.14**	1.24	−0.049***	−0.070**	−0.102
	SSI	$5.1 \bullet 10^{-4}$	$6.6 \bullet 10^{-4}$	$1.5 \bullet 10^{-3}$**	$-2.2 \bullet 10^{-5}$	$-3.2 \bullet 10^{-5}$	$-5.4 \bullet 10^{-5}$

Note: The dependent variables are the column headings. Data are displayed as slope and statistical significance: ***$P \leq 0.001$, **$P \leq 0.01$, *$P \leq 0.05$. IOP: intraocular pressure; MAP: mean arterial pressure; SSI: signal strength index.

Table 4. Mean vessel density (VD) and intercapillary distance (ICD) among sectors.

Sectors	VD (%)			ICD (mm)		
	SVC	GCLP	DCP	SVC	GCLP	DCP
1	0.438	0.439	0.441	0.021	0.021	0.021
2	0.442	0.443	0.439	0.021	0.021	0.021
3	0.438	0.441	0.442	0.022	0.021	0.020
4	0.421	0.425	0.445	0.023	0.022	0.020
5	0.380	0.382	0.323	0.025	0.025	0.028
6	0.329	0.330	0.278	0.029	0.029	0.031
7	0.333	0.334	0.273	0.029	0.029	0.031
8	0.381	0.383	0.313	0.025	0.025	0.029
9	0.420	0.423	0.440	0.022	0.022	0.021
10	0.435	0.436	0.436	0.022	0.021	0.021
11	0.445	0.443	0.437	0.021	0.021	0.021
12	0.439	0.440	0.442	0.021	0.021	0.021

Note: In the sectors that include more of the temporal region (5–8), there is a lower VD and higher ICD compared to the other sectors.
DCP: deep capillary plexus; GCLP: ganglion cell layer plexus; SVC: superficial vascular complex.

Table 5. No statistical significance in most comparisons looking at corresponding sectors above and below the horizontal.

Sectors	VD			ICD		
	SVC	GCLP	DCP	SVC	GCLP	DCP
1 vs. 12	0.91	0.69	0.75	0.41	0.34	0.35
2 vs. 11	0.58	0.88	0.86	0.67	0.63	0.43
3 vs. 10	0.31	0.22	0.33	0.45	0.28	0.045
4 vs. 9	0.98	0.55	0.37	0.52	0.28	0.065
5 vs. 8	0.68	0.86	0.12	0.61	0.67	0.008
6 vs. 7	0.22	0.23	0.17	0.79	0.83	0.24

Note: Data are displayed as *P* values from Wilcoxon rank sum tests comparing sectors.
DCP: deep capillary plexus; GCLP: ganglion cell layer plexus; ICD: intercapillary distance; SVC: superficial vascular complex; VD: vessel density.

strong test-retest reliability. To our knowledge, this is the first study of its size to investigate the far temporal region and provide normative OCTA data using an SD-OCTA device.

The transverse variation in VD and ICD in the plexuses studied here should be recognized. As the distance from the fovea increases temporally, VD decreases and ICD increases—agreeing with trends found in an SS-OCTA study.[17] In sectors 6 and 7, the Pearson correlation coefficients of the SVC and GCLP layers have a greater magnitude than that of the DCP layer—meaning that the decrease in VD is more prominent in superficial layers (Table 6). Alternatively, the deeper layers are more resistant to temporal and nasal variation. The VD map (Figure 3) corroborates this trend visually. With this in mind, caution should be exercised when defining the threshold for a pathologic decrease in VD of the temporal region. Going from the fovea towards the optic nerve head, both the SVC and GCLP VD increase while the DCP VD decreases.

The superior and inferior variations in VD and ICD are grossly symmetric above and below the horizontal in all vascular layers, as shown in the VD and ICD maps

Table 6. Regional variation analysis showing a decrease in vessel density and an increase in intercapillary distance towards the temporal region (sectors 5–8).

Sectors	Vessel density			Intercapillary distance		
	SVC	GCLP	DCP	SVC	GCLP	DCP
1	0.486***	0.405***	−0.376***	−0.323***	−0.293***	0.348***
2	0.471***	0.347***	−0.420***	−0.276***	−0.238***	0.376***
3	0.300***	0.258***	−0.441***	−0.294***	−0.300***	0.325***
4	−0.082	−0.102	−0.466***	0.065	0.018	0.441***
5	−0.447***	−0.478***	−0.370***	0.416***	0.438***	0.322***
6	−0.718***	−0.722***	−0.399***	0.533***	0.545***	0.200***
7	−0.746***	−0.747***	−0.467***	0.549***	0.545***	0.306***
8	−0.520***	−0.524***	−0.510***	0.498***	0.521***	0.496***
9	0.002	−0.015	−0.466***	0.129*	0.102	0.481***
10	0.197***	0.067	−0.547***	−0.042	−0.008	0.426***
11	0.550***	0.351***	−0.470***	−0.273***	−0.201***	0.407***
12	0.572***	0.483***	−0.340***	−0.320***	−0.269***	0.402***

Note: The correlations of vessel density and intercapillary distance with increasing foveal distance in sectors are reported as Pearson correlation coefficients and statistical significance: ***$P \leq 0.001$, *$P \leq 0.05$. The dependent variables are the column headings.
DCP: deep capillary plexus; GCLP: ganglion cell layer plexus; SVC: superficial vascular complex.

Table 7. Repeatability analysis using intraclass correlation coefficients (two-way mixed-effects model) in a subset of 25 eyes showing moderate to excellent reliability of both vessel density (VD) and intercapillary distance (ICD) in all layers.

		ICC	CI	*P* value
VD	SVC	0.93	[0.86, 0.96]	<0.001
	GCLP	0.91	[0.83, 0.95]	<0.001
	DCP	0.84	[0.70, 0.91]	<0.001
ICD	SVC	0.80	[0.64, 0.89]	<0.001
	GCLP	0.81	[0.66, 0.90]	<0.001
	DCP	0.64	[0.40, 0.80]	<0.001

CI: confidence interval; DCP: deep capillary plexus; GCLP: ganglion cell layer plexus; ICC: intraclass correlation coefficient; SVC: superficial vascular complex.

(Figure 3). In most comparisons, there is no significant difference between the vertically symmetric sectors (Table 4). This demonstrates that the VD and ICD remain relatively constant in the superior and inferior directions within 6-mm of the horizontal.

Based on multiple linear regression, the SSI should be corrected for in the DCP. This finding supports prior studies describing the impact of SSI on quantitative measures of vessel density in OCTA.[23–25] In most of our regression models, age was not correlated with VD or ICD despite a similar distribution of age compared to previous reports concluding vessel density decreased with age.[26,27] The relationship between vessel density and blood pressures has not been fully elucidated. However, studies have agreed that intraocular pressures up to 20 mmHg showed no impact on macular VD.[28,29] This may help to explain the intraocular and mean arterial pressure findings in the regression models. For example, an increase in mean arterial pressure correlated with a decrease in VD only in the macular region.

As the distance from the fovea increased, all layers became thinner (Figure 3) though the change in the DCP was less drastic compared to both the SVC and GCLP. Additionally, we reported that the retinal thickness in the temporal region was significantly lower compared to that of the macular region just as vessel density also decreased in the temporal region, agreeing with previous studies.[30,31] However, the multiple linear regression analysis only captured this relationship in some models. For example, only in DCP in the *temporal* region (not the macular region) did an increase in thickness correlate with an increase in VD and a decrease in ICD (Table 3). In contrast, in both the SVC and GCLP layers of the *macular* region only (not the temporal region), an increased thickness was associated with an increase in VD and a decrease in ICD.

Based on the repeatability analysis of a subset of the data, VD measurements exhibited excellent reliability in SVC and GCLP and good reliability in the DCP. Our VD results agree well with previously published reports.[32,33] ICD measurements demonstrated good reliability in SVC and GCLP and moderate reliability in the DCP.

There are a few limitations to note in this study. We did not examine the intermediate capillary plexus (ICP) in this work due to inadequate image quality in a number of images. The image resolution was also not sufficient to show the axial capillary density profiles to visualize density by depth in each vascular layer. Additionally, minor vignetting of images in the maps (lower VD and higher ICD at the corners) are present, which can have three causes. First, at the nasal corner of the image, the slight vignetting may cause a reduction of the flow signal in the DCP. Second, the thickened nerve fiber layer at the corner may lead to a weaker signal in the deeper layers, which manifests as an increase in SVC VD and a decrease in DCP VD. Lastly, the shadows caused by large vessels in the superficial layers, and the shadow caused by the large vessels may affect the signal strength of deeper capillaries.

In conclusion, we have characterized the VD and ICD wide-field temporal/macular OCTA images in a healthy population. The ICD increases and VD decreases towards the temporal region—with the superficial layers exhibiting a larger change. Based on multiple linear regression models, SSI exhibited significant correlations to VD and

ICD measurements in the DCP layer, and correction for this should be considered. Lastly, we showed the moderate to excellent reliability of both VD and ICD measurements. These trends will hopefully provide useful normative data for interpreting vascular metrics obtained with wide-field OCTA.

AUTHORS' CONTRIBUTIONS

All authors participated in the design, interpretation of the studies and analysis of the data and review of the manuscript. KL and TH wrote the manuscript, and YJ and TSH reviewed the manuscript.

DECLARATION OF CONFLICTING INTERESTS

Jia has a significant financial interest in Optovue Inc., a company that may have a commercial interest in the results of this research and technology. These potential conflicts of interest have been reviewed and managed by OHSU. No other disclosures were reported.

FUNDING

ORCID iDs

Yukun Guo https://orcid.org/0000-0002-6784-2355
Tristan Hormel https://orcid.org/0000-0002-7242-1934
Yali Jia https://orcid.org/0000-0002-2784-1905

REFERENCES

1. Hwang TS, Jia Y, Gao SS, Bailey ST, Lauer AK, Flaxel CJ, Wilson DJ, Huang D. Optical coherence tomography angiography features of diabetic retinopathy. *Retina* 2015;**35**:2371–6
2. Kashani AH, Chen C-L, Gahm JK, Zheng F, Richter GM, Rosenfeld PJ, Shi Y, Wang RK. Optical coherence tomography angiography: a comprehensive review of current methods and clinical applications. *Prog Retin Eye Res* 2017;**60**:66–100
3. de Carlo TE, Romano A, Waheed NK, Duker JS. A review of optical coherence tomography angiography (OCTA). *Int J Retina Vitreous* 2015;**1**:5
4. Hormel TT, Jia Y, Jian Y, Hwang TS, Bailey ST, Pennesi ME, Wilson DJ, Morrison JC, Huang D. Plexus-specific retinal vascular anatomy and pathologies as seen by projection-resolved optical coherence tomographic angiography. *Prog Retin Eye Res* 2021;**80**:100878
5. Nesper PL, Roberts PK, Onishi AC, Chai H, Liu L, Jampol LM, Fawzi AA. Quantifying microvascular abnormalities with increasing severity of diabetic retinopathy using optical coherence tomography angiography. *Invest Ophthalmol Vis Sci* 2017;**58**:BIO307–15
6. Agemy SA, Scripsema NK, Shah CM, Chui T, Garcia PM, Lee JG, Gentile RC, Hsiao Y-S, Zhou Q, Ko T, Rosen RB. Retinal vascular perfusion density mapping using optical coherence tomography angiography in normals and diabetic retinopathy patients. *Retina* 2015;**35**:2353–63
7. Hwang TS, Gao SS, Liu L, Lauer AK, Bailey ST, Flaxel CJ, Wilson DJ, Huang D, Jia Y. Automated quantification of capillary nonperfusion using optical coherence tomography angiography in diabetic retinopathy. *JAMA Ophthalmol* 2016;**134**:367–73
8. Ishibazawa A, Nagaoka T, Takahashi A, Omae T, Tani T, Sogawa K, Yokota H, Yoshida A. Optical coherence tomography angiography in diabetic retinopathy: a prospective pilot study. *Am J Ophthalmol* 2015;**160**:35–44.e1
9. Sandhu HS, Eladawi N, Elmogy M, Keynton R, Helmy O, Schaal S, El-Baz A. Automated diabetic retinopathy detection using optical coherence tomography angiography: a pilot study. *Br J Ophthalmol* 2018;**102**:1564–9
10. Zhang S, Wu C, Liu L, Jia Y, Zhang Y, Zhang Y, Zhang H, Zhong Y, Huang D. Optical coherence tomography angiography of the peripapillary retina in primary Angle-Closure glaucoma. *Am J Ophthalmol* 2017;**182**:194–200
11. Lommatzsch C, Rothaus K, Koch JM, Heinz C, Grisanti S. Vessel density in OCT angiography permits differentiation between normal and glaucomatous optic nerve heads. *Int J Ophthalmol* 2018;**11**:835–43
12. Russell JF, Flynn HW, Sridhar J, Townsend JH, Shi Y, Fan KC, Scott NL, Hinkle JW, Lyu C, Gregori G, Russell SR, Rosenfeld PJ. Distribution of diabetic neovascularization on ultra-widefield fluorescein angiography and on simulated widefield OCT angiography. *Am J Ophthalmol* 2019;**207**:110–20
13. Alibhai AY, De Pretto LR, Moult EM, Or C, Arya M, McGowan M, Carrasco-Zevallos O, Lee B, Chen S, Baumal CR, Witkin AJ, Reichel E, de Freitas AZ, Duker JS, Fujimoto JG, Waheed NK. Quantification of retinal capillary nonperfusion in diabetics using wide-field optical coherence tomography angiography. *Retina* 2020;**40**:412–20
14. Chu Z, Zhang Q, Gregori G, Rosenfeld PJ, Wang RK. Guidelines for imaging the choriocapillaris using OCT angiography. *Am J Ophthalmol* 2021;**222**:92–101
15. Chan G, Balaratnasingam C, Xu J, Mammo Z, Han S, Mackenzie P, Merkur A, Kirker A, Albiani D, Sarunic MV, Yu D-Y. In vivo optical imaging of human retinal capillary networks using speckle variance optical coherence tomography with quantitative clinico-histological correlation. *Microvasc Res* 2015;**100**:32–9
16. You QS, Chan JCH, Ng ALK, Choy BKN, Shih KC, Cheung JJC, Wong JKW, Shum JWH, Ni MY, Lai JSM, Leung GM, Cheung CMG, Wong TY, Wong IYH. Macular vessel density measured with optical coherence tomography angiography and its associations in a large population-based study. *Invest Ophthalmol Vis Sci* 2019;**60**:4830–7
17. Lavia C, Mecê P, Nassisi M, Bonnin S, Marie-Louise J, Couturier A, Erginay A, Tadayoni R, Gaudric A. Retinal capillary plexus pattern and density from fovea to periphery measured in healthy eyes with Swept-Source optical coherence tomography angiography. *Sci Rep* 2020;**10**:1474
18. Guo Y, Camino A, Zhang M, Wang J, Huang D, Hwang T, Jia Y. Automated segmentation of retinal layer boundaries and capillary plexuses in wide-field optical coherence tomographic angiography. *Biomed Opt Express* 2018;**9**:4429–42
19. Hormel TT, Wang J, Bailey ST, Hwang TS, Huang D, Jia Y. Maximum value projection produces better en face OCT angiograms than mean value projection. *Biomed Opt Express* 2018;**9**:6412–24
20. Campbell JP, Zhang M, Hwang TS, Bailey ST, Wilson DJ, Jia Y, Huang D. Detailed vascular anatomy of the human retina by Projection-Resolved optical coherence tomography angiography. *Sci Rep* 2017;**7**:42201
21. Maurer CR, Rensheng Q, Raghavan V. A linear time algorithm for computing exact Euclidean distance transforms of binary images in arbitrary dimensions. *IEEE Trans Pattern Anal Mach Intell* 2003;**25**:265–70
22. Guo Y, Hormel TT, Xiong H, Wang B, Camino A, Wang J, Huang D, Hwang TS, Jia Y. Development and validation of a deep learning algorithm for distinguishing the nonperfusion area from signal reduction artifacts on OCT angiography. *Biomed Opt Express* 2019;**10**:3257–68
23. Lim HB, Kim YW, Kim JM, Jo YJ, Kim JY. The importance of signal strength in quantitative assessment of retinal vessel density using optical coherence tomography angiography. *Sci Rep* 2018;**8**:12897

24. Rao HL, Pradhan ZS, Weinreb RN, Reddy HB, Riyazuddin M, Sachdeva S, Puttaiah NK, Jayadev C, Webers CAB. Determinants of peripapillary and macular vessel densities measured by optical coherence tomography angiography in normal eyes. *J Glaucoma* 2017;**26**:491–7

25. Venugopal JP, Rao HL, Weinreb RN, Pradhan ZS, Dasari S, Riyazuddin M, Puttiah NK, Rao DAS, Devi S, Mansouri K, Webers CA. Repeatability of vessel density measurements of optical coherence tomography angiography in normal and glaucoma eyes. *Br J Ophthalmol* 2018;**102**:352–7

26. Wu J, Sebastian RT, Chu CJ, McGregor F, Dick AD, Liu L. Reduced macular vessel density and capillary perfusion in glaucoma detected using OCT angiography. *Curr Eye Res* 2019;**44**:533–40

27. Yu JJ, Camino A, Liu L, Zhang X, Wang J, Gao SS, Jia Y, Huang D. Signal strength reduction effects in OCT angiography. *Ophthalmol Retina* 2019;**3**:835–42

28. Ma Z, Qiu W, Zhou D, Yang W, Pan X, Chen H. Changes in vessel density of the patients with narrow antenior chamber after an acute intraocular pressure elevation observed by OCT angiography. *BMC Ophthalmol* 2019;**19**:132

29. Zhang Q, Jonas JB, Wang Q, Chan SY, Xu L, Wei WB, Wang YX. Optical coherence tomography angiography vessel density changes after acute intraocular pressure elevation. *Sci Rep* 2018;**8**:6024

30. Milani P, Montesano G, Rossetti L, Bergamini F, Pece A. Vessel density, retinal thickness, and choriocapillaris vascular flow in myopic eyes on OCT angiography. *Graefes Arch Clin Exp Ophthalmol* 2018;**256**:1419–27

31. She X, Guo J, Liu X, Zhu H, Li T, Zhou M, Wang F, Sun X. Reliability of vessel density measurements in the peripapillary retina and correlation with retinal nerve fiber layer thickness in healthy subjects using optical coherence tomography angiography. *Ophthalmologica* 2018;**240**:183–90

32. Al-Sheikh M, Tepelus TC, Nazikyan T, Sadda SR. Repeatability of automated vessel density measurements using optical coherence tomography angiography. *Br J Ophthalmol* 2017;**101**:449–52

33. Lei J, Durbin MK, Shi Y, Uji A, Balasubramanian S, Baghdasaryan E, Al-Sheikh M, Sadda SR. Repeatability and reproducibility of superficial macular retinal vessel density measurements using optical coherence tomography angiography en face images. *JAMA Ophthalmol* 2017;**135**:1092–8